Available online at www.sciencedirect.com

SCIENCE DIRECT®

Thermochimica Acta 431 (2005) 87–93

thermochimica acta

www.elsevier.com/locate/tca

Phase behavior of banana-shaped molecules under pressure

Yoji Maeda[a, *], Teruki Niori[b], Jun Yamamoto[b], Hiroshi Yokoyama[b]

[a] Nanotechnology Research Institute, National Institute of Advanced Industrial Science and Technology, Higashi 1-1, Tsukuba, Ibaraki 305-8565, Japan
[b] Yokoyama Nano-structured Liquid Crystal Project, JST, Tsukuba, Ibaraki 300-2635, Japan

Received 20 October 2004; received in revised form 14 December 2004; accepted 20 January 2005
Available online 19 February 2005

Abstract

The phase transition behavior of two achiral bent core banana-shaped molecules, 3- and 3-(3′-chloro-)(4′-*n*-octyloxybenzoyloxyphenyliminomethyl)phenyl-4″-*n*-octyloxy biphenylcarboxylate (**I** and **II**), showing the B_1 and B_2 banana phases, respectively, was investigated under hydrostatic pressures up to 300 MPa using a high-pressure differential thermal analyzer. The T versus P phase diagrams for **I** and **II** compounds were constructed. Both the temperature regions of the B_1 and B_2 phases for **I** and **II** compounds are maintained in the whole pressure range and the B_1 and B_2 phases are thermodynamically stable under pressures.

Keywords: Banana-shaped liquid crystals; High-pressure DTA; T–P phase diagram; B_1 and B_2 phases; High-pressure crystal phase

1. Introduction

Banana-shaped liquid crystals, different from conventional calamitic liquid crystals, have been extensively studied since Niori et al. [1–5] reported on ferroelectricity in a smectic phase formed by banana-shaped Schiff-base derivatives in 1996. As a consequence of the bent molecular shapes, a polar packing of the molecules within smectic layers gives rise to several new mesophases labeled by the code letters B_n [6–8]. These mesophases are not compatible with the conventional SmA and SmC phases.

Despite numerous studies have been made on banana-shaped molecules for about 10 years, the studies on phase behavior of bent-core molecules under pressure are very few. It is found that the two-dimensionally ordered B_1 and B_2 phases are stable in the pressure region up to 200–300 MPa [9,10]. Weissflog et al. [9] reported an interesting thermal behavior of the *N*,*N*′-bis[4-(4-*n*-octyloxybenzoyloxy) benzylidene]phenylene-1,3-diamine with the B_1 phase and its phase diagram: at higher pressures two transition peaks appear reversibly below the clearing point and a new high-pressure phase, denoted as Cr_2, is found. They determined a triple point (84 MPa, 135 °C) for the Cr_1, Cr_2 and B_1 phases, indicating the lower limit of pressure for the high-pressure Cr_2 phase. Krishna Prasad et al. [10] reported the phase behavior of two achiral banana-shaped molecules, hexyloxy and decyloxy members of 1,3-phenylene bis[*N*-(2-hydroxy-4-*n*-alkoxybenzylidene)-4′-aminobenzoate] under pressures up to 300 MPa. The reversible transition sequence Cr_1–B_1–I for the hexyloxy compound, observed at atmospheric pressure, remains in the pressure region up to ca. 70 MPa, while a pressure-induced crystal phase (Cr_i) appears between the Cr_1 and B_1 phases under higher pressures. The phase diagram includes a triple point (73 MPa and 160 °C) for the Cr_1, Cr_i and B_1 phases. On the other hand, the reversible transition sequence Cr_1–B_2–I of the decyloxy compound occurs under all pressures studied. Both the B_1 and B_2 banana phases are thermodynamically stable under whole pressures.

In this paper, we present the experimental results of the thermal behavior of 3-(4′-*n*-octyloxybenzoyloxyphenyliminomethyl)phenyl-4″-*n*-octyloxy biphenylcarboxy-

---

[*] Corresponding author. Tel.: +81 29 861 6282; fax: +81 29 861 6282.
E-mail address: yoji.maeda@aist.go.jp (Y. Maeda).

doi:10.1016/j.tca.2005.01.047

late (compound **I**) and 3-(3′-chloro-)derivative (compound **II**) under hydrostatic pressures up to 300 MPa using a high-pressure differential thermal analyzer (DTA). The chemical structures of the compounds **I** and **II** are shown below.

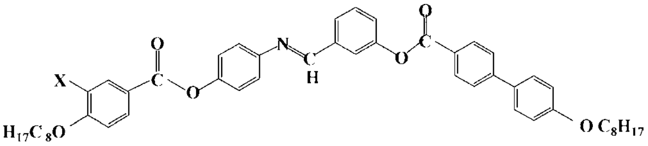

X = H : I
Cl : II

2. Experimental

2.1. Sample preparation and characterization

The synthesis of the banana-shaped molecules studied here is described in elsewhere [11]. The two compounds were characterized by using a Perkin-Elmer DSC-7 differential scanning calorimeter (DSC), a Leitz Orthoplan polarizing optical microscope (POM), and a Rigaku Rotaflex RU-200 wide-angle X-ray diffractometer (WAXD). DSC measurements were performed at a scanning rate of 5 °C min^{-1} under N_2 gas flow. Temperatures and heats of transition were calibrated using the standard materials, indium and tin. Transition temperatures were determined as the onset of the transition peaks at which the tangential line of the inflection point of the rising part of the peak crosses over the extrapolated baseline. Texture observation was performed using a POM equipped with a Mettler hot stage FP-82 and with a high-pressure optical cell [12]. Ni-filtered Cu Kα X-ray irradiation ($\lambda = 1.542$ Å) and an imaging plate detector (BAS-IP 127 mm × 127 mm, Fuji Photo Film Co.) was used for the X-ray diffraction patterns of the crystals and two banana phases of the **I** and **II** compounds.

2.2. DTA measurements under pressure

The high-pressure DTA apparatus used in this study is described elsewhere [13]. The DTA system was operated in a temperature region between room temperature and 250 °C under hydrostatic pressures up to 300 MPa. Dimethylsilicone oil with a medium viscosity (100 cSt) was used as the pressurizing medium. The sample weighing about 4 mg was put in the sample cell and coated with epoxy adhesives, to fix the sample in the cell and also to prevent direct contact with the silicone oil. In the DTA measurements new sample was used for each DTA measurement. The DTA runs were performed at a constant scanning rate of 5 °C min^{-1} under various pressures. Peak temperature was adopted usually as transition temperature.

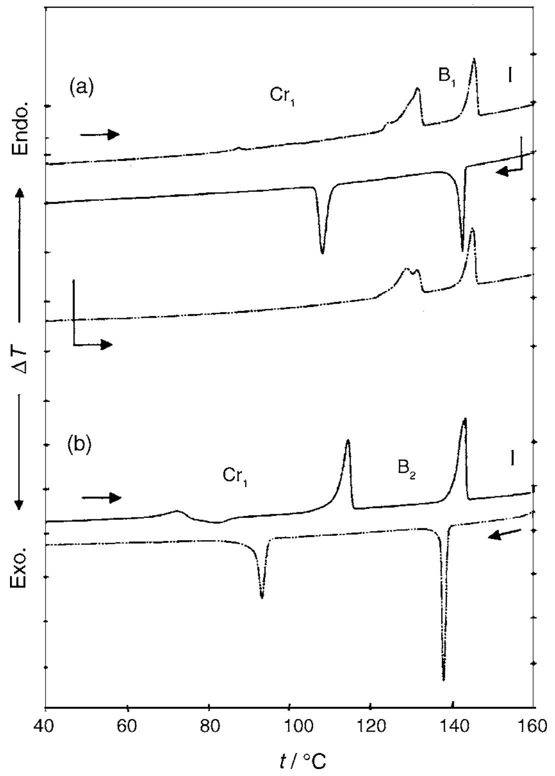

Fig. 1. DSC curves of compounds **I** and **II** at a scanning rate of 5 °C min^{-1}: (a) heating and cooling runs for compound **I** and (b) cooling and subsequent heating runs for compound **II**.

3. Results and discussion

3.1. Phase behavior at ambient pressure

Fig. 1 shows the DSC heating and cooling curves of **I** and **II** compounds at a scanning rate of 5 °C min^{-1}. Both compounds show a simple thermal behavior: two peaks of melting and isotropization. The thermodynamic quantities associated with the phase transitions for the two compounds are listed in Table 1.

The mesophases are assigned by their optical textures and X-ray diffraction as B_1 phase for compound **I** and B_2 phase for compound **II** (chloro-derivative). Fig. 2 shows the typical POM photographs of the B_1 and B_2 textures observed on cooling for the compounds **I** and **II**, respectively. Compound **I** exhibits a mosaic texture, characteristic of the B_1 phase, while compound **II** shows a spherulitic growth for the B_2 phase. The B_1 phases grow usually as dendritic nuclei which coalesce to a mosaic texture [7]. On the other hand, the B_2 phase shows spherulitic texture.

The X-ray patterns of the B_1 phase of compound **I** show two sharp reflections in the small angle region, while a diffuse scattering in the wide-angle region. This pattern could be explained by a two-dimensional rectangular or columnar rectangular cell (Col_r) by Watanabe et al.'s model [14]. Scheme 1 illustrates the molecular packing in frustrated structures of the B_1 and B_2 phases [7,9,14]. According to the two-

Table 1
Thermodynamic quantities associated with the phase transitions for compounds **I** and **II**, Prasad et al.'s and Weissflog et al.'s compounds for comparison

	T (°C)	ΔH (kJ mol^{-1})	ΔS (J K^{-1} mol^{-1})	dT/dP (K MPa^{-1})	ΔV* (cm^3 mol^{-1})
Compound **I** ($n = 8$)					
Cr_1–B_1	128.4	26.0	64.7	0.31_5	20.4
B_1–I	143.7	20.5	49.2	0.34_1	16.8
Compound **II** ($n = 8$)					
Cr_1–B_2	111.4	21.5	55.9	0.28_7	16.1
B_2–I	141.0	20.1	48.5	0.29_4	14.3
(1) Prasad et al.'s compound ($n = 6$)[a]					
Cr_1–B_1	143.4	37.2	89.3	0.17_5	15.7
B_1–I	175.3	16.7	37.2	0.28_0	10.4
Prasad et al.'s compound **II** ($n = 10$)[a]					
Cr_1–B_2	117.5	22.7	58.2	0.28_9	16.8
B_2–I	180.0	24.5	54.1	0.29_9	16.2
(2) Weissflog et al.'s compound ($n = 8$)[b]					
Cr_1–B_1	112	25.6	66.5	0.30_3	20.1
B_1–I	132	16.3	40.2	0.36_8	14.8

[a]

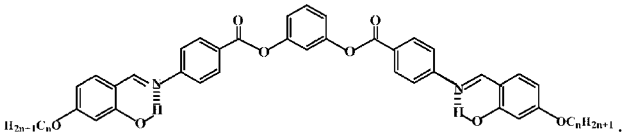

[b]

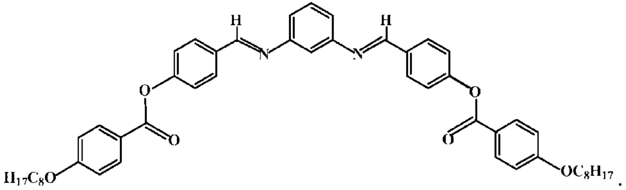

dimensional rectangular cell, the length of c-axis, i.e., layer thickness, corresponds to the molecular length, and the frustration, i.e., unusual density modulation, takes place along the a-axis and the bent direction of molecules is in the a-axis. The density modulation in the a-axis is produced by the periodic structure with inversion domain walls such that the molecules in an adjacent domain slide halfway along the layer normal after 180° rotation around the molecular axis. The unit length of the a-axis includes 8–10 molecules, on average, and then 4 or 5 molecules in each domain [14]. Accordingly the two sharp reflections in the small-angle region may correspond to the (1 0 1) and (0 0 2) reflections of the B_1 phase of compound **I**. On the other hand, the X-ray pattern of the B_2 phase shows only one reflection in the small angle region, corresponding to the layer thickness of the B_2 phase. The B_2 phase is more precisely described as $SmCP_A$, a tilted smectic phase (SmC) with a polar order of the molecules (P) within the layers and an antiferroelectric interlayer correlation. The d-spacings estimated from the reflections are listed in Table 2. The d-spacings of the B_1 and B_2 phases are comparable to those of the B_1 and B_2 phases of other banana-shaped molecules [14,15].

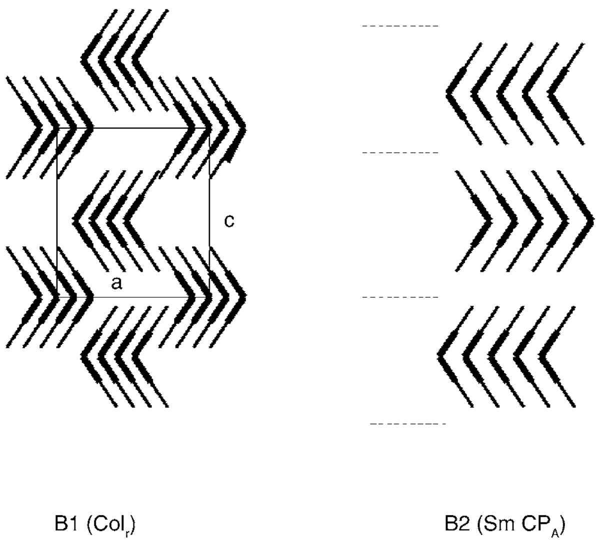

Scheme 1. Schematic drawings of the molecular packing of B_1 and B_2 phases.

3.2. Phase behavior under pressure

Fig. 3 shows the DTA heating curves of compound **I** at various pressures. Since the DTA curves are generally noisy with large S/N ratio, only the transition peaks are discussed in this study. The heating curves at 50, 100 and 280 MPa show two endothermic peaks of the Cr_1–B_1 and B_1–I transitions. The Cr_1–B_1–I transition sequence, observed at atmospheric pressure (see Fig. 1), is maintained in the whole pressure range studied. Fig. 4 shows the DTA heating curves

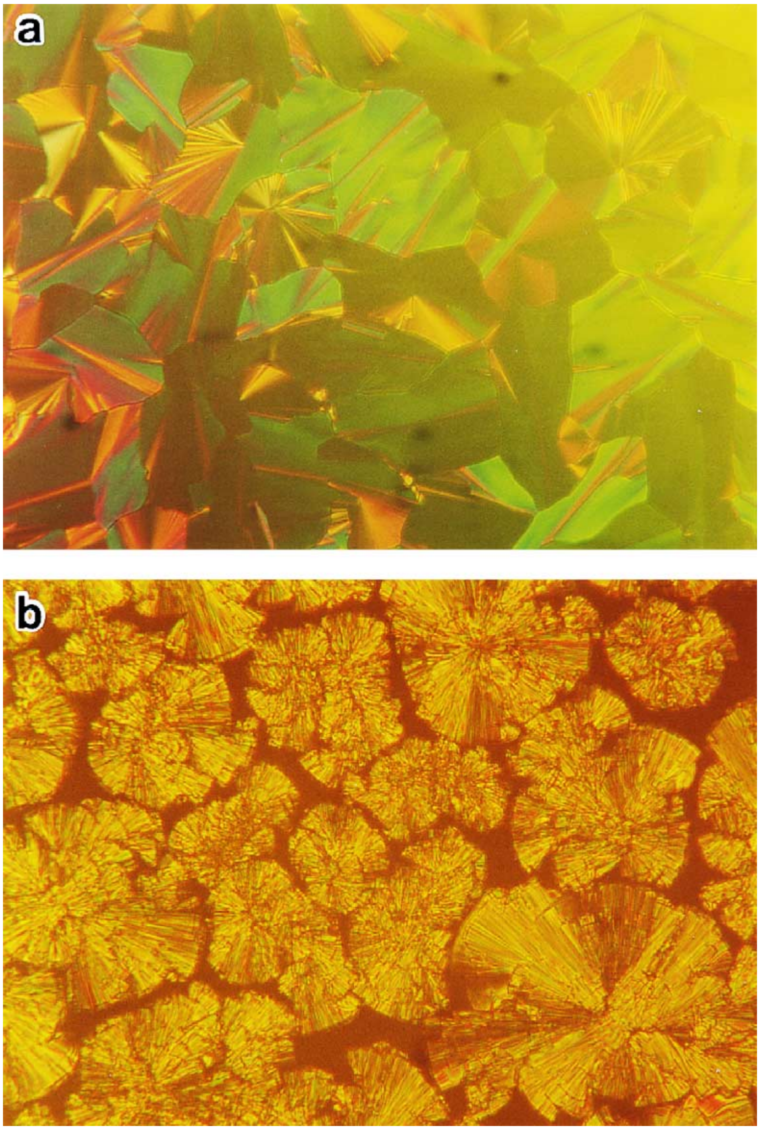

Fig. 2. POM photographs of the textures of (a) the B_1 phase of compound **I** at 141 °C and (b) the B_2 phase of compound **II** at 139 °C, respectively.

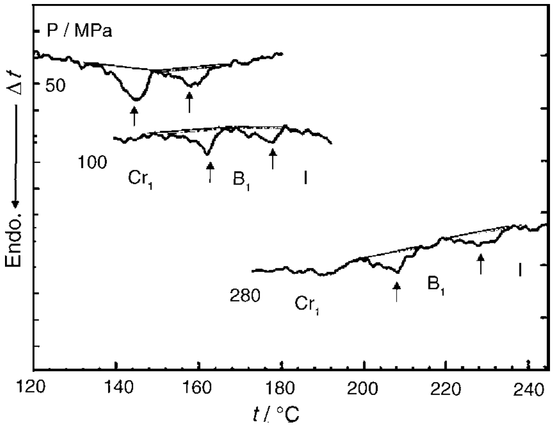

Fig. 3. DTA heating curves of compound **I** at indicated pressures. Heating rate: 5 °C min^{-1}.

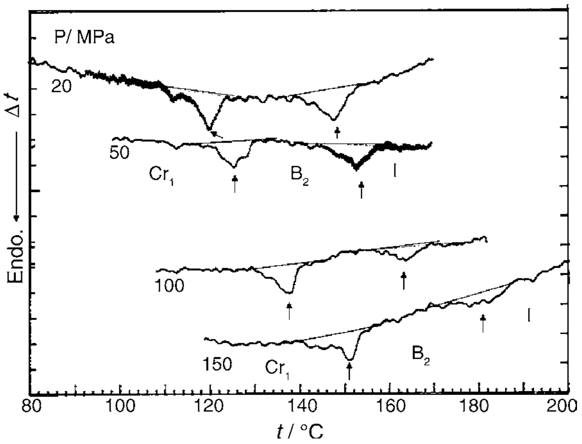

Fig. 4. DTA heating curves of compound **II** at indicated pressures. Heating rate: 5 °C min^{-1}.

Table 2
Data of *d*-spacing calculated from the X-ray reflections of the crystalline, B_1 and B_2 phases for the banana-shaped molecules **I** and **II**

d-spacing (nm) (2*θ*, °)	
Crystalline phase 24 °C	Banana phase 130 °C
Cr	B_1 phase
Compound **I**	
3.74 (2.36°)	2.81 (3.14°)
2.01 (4.39°)	1.97 (4.48°)
0.43 (20.6°)	
Cr	B_2 phase
Compound **II**	
3.68 (2.40°)	3.47 (2.54°)
1.82 (4.84°)	
0.42 (20.9°)	

of compound **II** under hydrostatic pressures up to 150 MPa. The thermal behavior is very similar to those of compound **I** under pressures, indicating the Cr_1–B_2 and B_2–I transitions, respectively. Fig. 5 shows the DTA heating curves of compound **II** at 200 and 300 MPa. Increasing the pressure above 150–200 MPa, however, splits the endothermic peak of melting into two peaks as shown in Fig. 5. The second one at a higher temperature is a small endothermic peak which is a little bigger than the noise signals. The first and second peaks are due to the major melting of the Cr_1 phase and some phase between the Cr_1 and B_2 phases, respectively. There are two possibilities for the phase: first one is a pressure-induced crystalline phase, which can be seen in other banana-shaped molecules [9,10]. Second one is an appearance of either another banana phase or other smectic phase. The existence of another crystalline phase seems to be more realistic, and in fact, it was attributed to a pressure-induced crystalline polymorph by direct WAXD measurements under pressure. The pressure-induced crystal phase is named here as Cr_i. So the Cr_1–B_2–I and Cr_1–Cr_i–B_2–I transition sequences of compound **II** can be seen in the low- and high-pressure regions above about 200 MPa, respectively.

Figs. 6 and 7 show the *T* versus *P* phase diagrams of compounds **I** and **II** in the pressure range up to 300 MPa, respectively. All of the phase transition lines can be approximated to be a first- or second-order polynomials of pressure as follows:

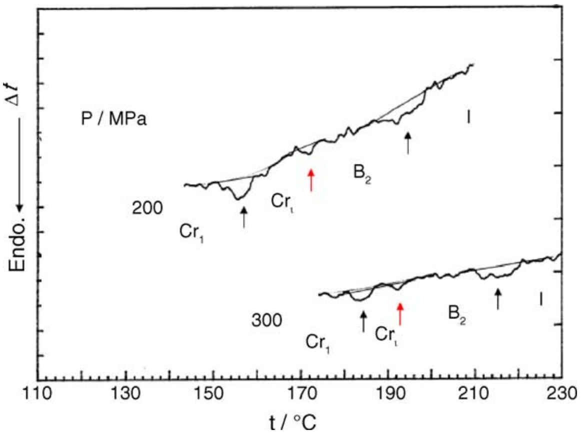

Fig. 5. DTA heating curves of compound **II** at 200 and 300 MPa.

	Whole pressures
Compound **I**	
Cr_1–B_1	$T = 132 + 0.31_5P - 1.7_9 \times 10^{-4}P^2$
B_1–I	$T = 145 + 0.34_1P - 1.7_5 \times 10^{-4}P^2$
Compound **II**	
$0 < P < 150$ MPa	
Cr_1–B_2	$T = 114 + 0.28_7P - 2.0_0 \times 10^{-4}P^2$
$P > 150$ MPa	
Cr_1–Cr_i	$T = 122 + 0.20_2P$
Cr_i–B_2	$T = 114 + 0.25_4P$
B_2–I	$T = 142 + 0.29_4P - 1.6_6 \times 10^{-4}P^2$

Generally the Cr_1–B_2 transition point of compound **II** is lower by about 18 °C than the Cr_1–B_1 transition point by changing the hydrogen atom to chlorine in the chemical structure of compound **I**. In the case of compound **I** the temperature region for the B_1 phase broadens gradually with increasing pressure, but the temperature region of about 28 °C of the B_2 phase is almost constant under all pressures because the pressure-induced crystal phase Cr_i appears between the Cr_1 and B_2 phases under elevated pressures. One can see that the Cr_1–Cr_i and Cr_i–B_2 transition lines merge at about 150 MPa, indicating the existence of a triple point (149 MPa, 152 °C) which suggests the lower limit of pressure for the Cr_i phase.

The existence of a triple point in the *T* versus *P* phase diagram for banana-shaped molecules are already found by Weissflog et al. [9] and Krishna Prasad et al. [10]: Weissflog et al. showed the *T* versus *P* phase diagram of *N*,*N*′-bis[4-(4-*n*-octyloxybenzoyloxy)benzylidene]phenylene-1,3-diamine, which exhibits the triple point at 84 MPa and 135 °C between the three stable phases, Cr_1, high-pressure crystal (Cr_2), and B_1 phases. Krishna Prasad et al. also exhibited the *T* versus *P* phase diagram of the hexyloxy compound which shows

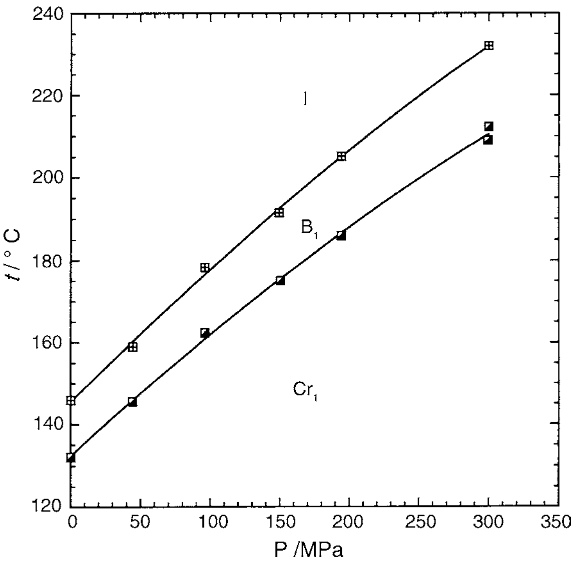

Fig. 6. *T* vs. *P* phase diagram for compound **I**.

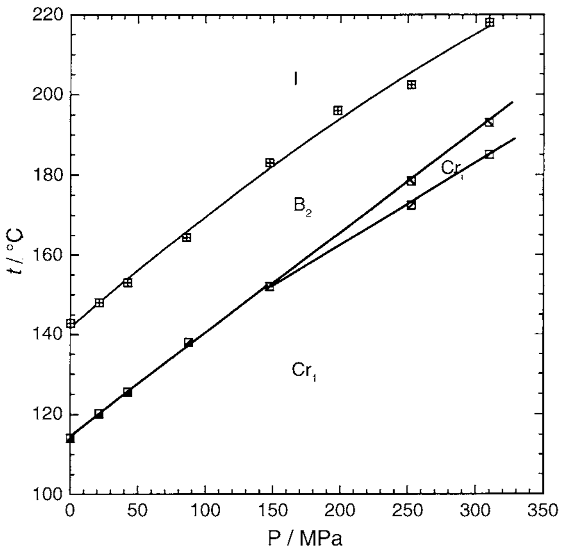

Fig. 7. T vs. P phase diagram for compound **II**.

the triple point at 73 MPa and 160 °C between the Cr_1, a pressure-induced crystal (Cr_i), and B_1 phases, indicating the lower limit of pressure for the Cr_i phase. The existence of a triple point for the Cr_1, Cr_i and B_2 phases seems to be the same phenomenon as those observed already, but it is not clear why the pressure-induced crystal phase appears often in the banana-shaped molecules.

The slight pressure dependence of the temperature range for the B_1 and B_2 phases is not so strange in banana-shaped liquid crystalline systems. The slopes (dT/dP: 0.31 and 0.34 °C/MPa) for the Cr_1–B_1 and B_1–I transitions and the values (0.29 °C/MPa) for the Cr_1–B_2 and B_2–I transitions of compounds **I** and **II** are surprisingly comparable to the results reported by Krishna Prasad et al. [10] although its chemical structure is different from the structure of **I** and **II** compounds in this study (see table). The values of the slopes also are comparable to the results (0.303 and 0.368 °C/MPa) for the Cr_1–B_1 and B_1–I transitions of Weissflog et al.'s *N*,*N*′-bis[4-(4-*n*-octyloxybenzoyloxy)benzylidene]phenylene-1,3-diamine [9]. They discussed the thermodynamic quantities for the Cr–B_1 and B_1–I transitions of the octyloxy ($n = 8$) compound which is the same spacer length at both ends of the molecule as **I** and **II** compounds in this study. Estimated on the Clausius–Clapeyron equation, the ΔH and ΔV values associated with the Cr_1–B_1 and B_1–I transitions are compared among three studies in Table 1. The transition enthalpies and entropies are comparable with each other, even if the chemical structures for the bent core of banana-shaped molecules are different. This suggests the substantial contribution to the transition enthalpies or entropies by the alkyloxy spacer groups at both ends of the banana-shaped molecules: especially the spacer length often may play the key contribution to the appearance of the B_n phases in the same bent core molecules. The similar relation exists in the B_2 phases between compound **II** and Prasad et al.'s decyloxy compound. Generally speaking, the ΔH values for the B_1 (or B_2)–I transitions are comparable with those for the Cr_1–B_1 (or B_2) transition and the values are 1–2 decades larger than the transition enthalpies (0.08–9.6 kJ mol^{-1}) for the nematic(N)–I transition of classical calamitic liquid crystals, but it is in the same order with the transition enthalpies (2.9–12.5 and 10.0–42.7 kJ mol^{-1}) for the SmA–I and SmC–I transitions, respectively [16–18]. It is interesting to compare the transition entropies with those for calamitic liquid crystals. The ΔS values are only 3.0 J K^{-1} mol^{-1} for the N–I transition of *p*-*n*-hexyloxybenzylidene-*p*′-toluidine [19], but 22.7 J K^{-1} mol^{-1} for the SmC–I transition of 1,2-bis(4-*n*-octyloxybenzoyl)hydrazine BABH(8) [20]. The ΔS values of the B_1 (or B_2)–I transition for I (or II) compounds in this study are 2 times larger than that for the SmC–I transition of BABH(8) compound. Table 1 indicates that this relation stands more or less in two other banana-shaped molecules. These experimental facts point to the high degree of order in the B_1 and B_2 phases, comparable with those of the classical SmC phases.

In summary the phase transition behavior of two banana-shaped bent core molecules was investigated under hydrostatic pressures up to 300 MPa using a high-pressure DTA method. Based on the experimental results it can be concluded that both the B_1 and B_2 banana phases are thermodynamically stable under elevated pressures studied.

References

[1] T. Niori, T. Sekine, J. Watanabe, T. Furukawa, H. Takezoe, J. Mater. Chem. 6 (1996) 1231.

[2] T. Niori, T. Sekine, J. Watanabe, T. Furukawa, H. Takezoe, Mol. Cryst. Liq. Cryst. 301 (1997) 337.

[3] T. Sekine, Y. Takanishi, T. Niori, J. Watanabe, H. Takezoe, Jpn. J. Appl. Phys. 36 (1997) L1201.

[4] T. Sekine, T. Niori, M. Sone, J. Watanabe, S.W. Choi, Y. Takanishi, H. Takezoe, Jpn. J. Appl. Phys. 36 (1997) 6455.

[5] T. Sekine, T. Niori, J. Watanabe, T. Furukawa, S.W. Choi, H. Takezoe, J. Mater. Chem. 7 (1997) 1307.

[6] G. Heppke, D. Krüerke, C. Löhning, D. Lötzsch, S. Rauch, N.K. Sharma, Freiburger Arbeitstagung Flüssige Kristalle, 1997. Freiburg (Poster P70).

[7] G. Pelzl, S.S. Diele, W. Weissflog, Adv. Mater. 11 (1999) 707.

[8] The nomenclature of the mesophases of the banana-shaped molecules as B1, B2, etc. was recommended at the Workshop "Banana-Shaped Liquid Crystals: Chirality by Achiral Molecules", Berlin, December 1997.

[9] W. Weissflog, I. Wirth, S. Diele, G. Pelzl, H. Schmalfuss, T. Schoss, A. Würflinger, Liq. Cryst. 28 (2001) 1603.

[10] S. Krishna Prasad, Y. Maeda, D.S. Shankar Rao, S. Anitha Nagamani, U.S. Hiremath, C.V. Yelamaggad, Liq. Cryst. 30 (2003) 1277.

[11] T. Niori, J. Yamamoto, H. Yokoyama, Mol. Cryst. Liq. Cryst. 411 (2004) 283.

[12] Y. Maeda, M. Koizumi, Rev. Sci. Instrum. 67 (1996) 2030;
Y. Maeda, M. Koizumi, Rev. High Pressure Sci. Technol. 7 (1998) 1532.

[13] Y. Maeda, H. Kanetsuna, Bul. Res. Inst. Polym. Tex. 149 (1985) 119;
Y. Maeda, Thermochim. Acta 163 (1990) 211.

[14] J. Watanabe, T. Niori, T. Sekine, H. Takezoe, Jpn. J. Appl. Phys. 37 (1998) L139.
[15] D. Shen, A. Pegenau, S. Diele, I. Wirth, C. Tschierske, J. Am. Chem. Soc. 122 (2000) 1593.
[16] J. Thoen, in: D. Demus, J. Goodby, G.W. Gray, H.W. Spiess, V. Vill (Eds.), Handbook of Liquid Crystals, vol. 1, Wiley-VCH, Weinheim, 1998, p. 311.
[17] D. Marzotko, D. Demus, Pramana Suppl. 1 (1975) 189;
D. Marzotko, D. Demus, Proceedings of the International Conf. Liq. Cryst, Bangalore, 1973.
[18] S. Chandrasekhar, Liquid Crystals, 2nd ed., Cambridge University Press, 1992, p. 15.
[19] K. Tsuji, M. Sorai, H. Suga, S. Seki, Mol. Cryst. Liq. Cryst. 90 (1982) 97.
[20] N. Morimoto, K. Saito, Y. Morita, K. Nakasuji, M. Sorai, Liq. Cryst. 26 (1999) 219.